Surprising minimisation of CO_2 emissions from a sandy loam soil over a rye growing period achieved by liming ($CaCO_3$)

Rousset Camille[A,B], Brefort Henri[A], Fonseca, Rafael Frederico[A], Guyerdet Guillaume[A], Bizouard Florian[A], Mustapha Arkoun[C], Hénault Catherine[A]

[A]Agroécologie, INRAE, Institut Agro, Univ. Bourgogne, Univ. Bourgogne Franche-Comté, F-21000 Dijon, France

[B]Integrative Agroecology, Agroscope, Reckenholzstrasse 191, 8046 Zurich, Switzerland

[C]Laboratoire de Nutrition Végétale, Agroinnovation International – TIMAC AGRO, Saint-Malo, France

Corresponding authors:

catherine.henault@inrae.fr ORCID number: 0000-0002-1210-2499

UMR AgroEcologie
17 rue Sully
BP 86510
21065 Dijon Cedex
France

Abstract

Agricultural liming is a common practice for improving acidic soils production, and is also considered as a lever for mitigating nitrous oxide emissions from soils. However, the benefit of liming in reducing soil greenhouse gas emissions (GHG) is conditioned by: (i) the evolution of the carbon of the calcium carbonates ($CaCO_3$) supplied, and (ii) the effect of $CaCO_3$ on the evolution of soil organic carbon (SOC). The literature presents contrasting effects of liming on inorganic- and SOC-derived CO_2 emissions. Current understanding of the

impact of liming on GHG emissions is limited by the lack of field data, and therefore requires further study.

In situ, we monitored the effect of two liming products (SC = synthetic $CaCO_3$ and MC = marine $CaCO_3$) on soil CO_2 emissions compared to control plots, during the growing season of a winter rye, using the static chamber method. Soil pH, N_2O emissions, mineral nitrogen content, soil moisture and temperature were measured during the experiment, as well as plant biomass and SOC (stock and composition) on the day of harvest.

Lime addition increased soil pH and kernel yield and significantly decreased soil CO_2 emission with on average a reduction of 3.74 and 3.94 mg C kg^{-1} d^{-1}, for the MC and SC addition respectively. SOC at harvest was not affected but its composition was modified by the limed treatments. Liming was also associated with a decrease in dissolved organic carbon losses in the soil. Further investigations must be carried out to better understand the mechanisms explaining these observations and to define conditions in which liming application could act as a potential lever for carbon storage. Finally, our results suggest that the IPCC principles, estimating an increase of CO_2 emissions linked to the C added by lime materials, may need to be re-examined in the future.

Keywords: CO_2 emissions, pH, Agricultural liming, C stabilisation

Introduction

The benefits of liming in mitigating soil acidification and increasing crop productivity have been known for centuries (Blum et al., 2017). However, the focus of agriculture now lies not solely on production but also on maintaining a healthy environment. Direct emissions from the agriculture, forestry and land-use sector comprise roughly 18% of global greenhouse gas (GHG) emissions (Ritchie et al., 2020) which contribute to global warming and climate change. The main GHGs involved in the agriculture sector include nitrous oxide (N_2O), carbon dioxide (CO_2) and methane (CH_4). Recently, research attention has focused on the effect of liming on soil gas fluxes (Wang et al., 2021). Soil liming has numerous far-reaching impacts on soil processes and function (Holland et al., 2018). One is linked to the denitrification process, considered as the major source of N_2O emissions and often associated with the so-called soil N_2O emission hotspots in agriculture (Kravchenko et al., 2017). Complete denitrification is also the only known terrestrial mechanism allowing the elimination of this gas (Jones et al., 2013). The liming of acidic soils has been proposed as a potential lever for promoting N_2O reduction and consequently mitigating soil N_2O emissions (Shaaban et al., 2015). Hénault et al. (2019) suggested a specific pH of 6.8 below which the N_2O reduction pathway is progressively inhibited. Nevertheless, the diverse impacts of liming on plant and soil processes may also cause CO_2 emissions. Therefore, the influence of liming products on the GHG balance of soils (N_2O and CO_2) is controversial (Wang et al., 2021).

Calcium carbonate ($CaCO_3$) has the potential to dissolve into CO_2 and be released into the atmosphere (Bertrand et al., 2007; Biasi et al., 2008; Dumale Jr et al., 2011). The dissolution of $CaCO_3$ can act as either a source or sink for CO_2, depending on whether the reaction occurs with strong acids such as nitric acid (HNO_3^-) or weak acids such as carbonic acids (H_2CO_3) (Hamilton et al., 2007). In a strong acidic environment, CO_2 is released when $CaCO_3$ reacts with protons which can be derived from nitrification processes (Equation 1).

$$CaCO_3 + 2HNO_3 \rightarrow Ca^{2+} + 2NO_3^- + CO_2 + H_2O \ \#(1)$$

However, when every mole of $CaCO_3$ reacts with carbonic acid (H_2CO_3) in soils, it yields two moles of carbonate materials (HCO_3^-), thus serving as a sink of CO_2 in soil (Equation 2 & 3).

$$CO_2 + H_2O \leftrightarrow H_2CO_3 \#(2)$$

$$CaCO_3 + H_2CO_3 \rightarrow Ca^{2+} + 2HCO_3^- \#(3)$$

The principle of the Intergovernmental Panel on Climate Change, basically states that one mole of CO_2 is generated for each mole of carbonate dissolved (IPCC, 2006). Nevertheless, this position which tends to overestimate CO_2 emissions is challenged by several authors (West and McBride, 2005; Hamilton et al., 2007).

Soil pH is also known as a key abiotic factor that regulates soil microbiological activity and structure (Dumale Jr et al., 2011; Grover et al., 2017). The increase of pH induced by liming is also expected to stimulate microbial activities, which in turn can increase the transformation of soil organic matter (SOM) (decomposition/mineralisation, turnover, Paradelo et al., 2015), with the production of more CO_2 (Fuentes et al., 2006). A recent laboratory study from Lochon et al. (2018) showed that the liming response of CO_2 production mirrored those of carbon (C) mineralization namely: an increase, associated with a concurrent increase in soil pH. Adding lime could therefore contribute to soil organic-derived CO_2 emissions by inducing a positive priming effect on SOC decomposition (Grover et al., 2021). While positive priming effects have been more generally demonstrated in the literature (Kunhikrishnan et al., 2016), liming may also have no influence on SOC (Bertrand et al., 2007; Fornara et al., 2011; Lochon et al., 2019) or a negative priming effect on SOC decomposition by strengthening the clay-organic matter bonds with the calcium (Ca^{2+}) of the liming material (Oades, 1984; Wuddivira and Camps-Roach, 2007).

While laboratory studies show mixed responses of CO_2 emissions and SOC pools to liming application, fewer studies have been conducted to quantify these liming effects in the field (Holland et al., 2018). Nonetheless, studies suggest that CO_2 emissions derived from liming application may be much lower under field conditions compared to laboratory conditions (Cho et al., 2019; Lochon et al., 2019). It is also reasonable to assume that the direction (increase or decrease) and magnitude of the effect of liming on CO_2 emissions depend on site-specific abiotic conditions such as initial soil C content (Dumale Jr et al., 2011) or temperature. Therefore, the effects of surface liming on the SOC pool and its consequences on CO_2 emissions are not clear and require further study to predict the net outcome of liming on the soil C balance and climate regulation service. The objectives of our one-year-field study were: (i) on a weekly basis, simultaneously monitor the evolution of CO_2 and N_2O emission rates after the application of two $CaCO_3$ products (marine and synthetic) using the closed-chamber method to determine whether the change in CO_2 emissions offsets the benefits of liming products in reducing N_2O; (ii) to collect information on SOC on the harvesting day, obtained through its chemical characterisation, in order to identify a potential explanation for the evolution of CO_2; and (iii) to observe the interaction of liming with the site-specific abiotic conditions of soil respiration, namely temperature and soil humidity.

Materials and methods

Site description and treatment

The experiment was conducted on a farm plot (< 2 ha) located in Fourches Village, Morvan region in France (47°15'38.369" N; 4°11'18.952" E) at an altitude of 558 m. The Morvan region is an old mountain massif with an average temperature of 9°C, an average rainfall of 1016 mm and a late spring.

Soil of the experimental field is classified as a Brunisol according to the NGI (National Geographic Institute). Based on a composite soil sample taken before liming application and made up with 10 soil cores randomly distributed in the farm plot, this soil has a sandy loam texture (60.8 % sand, 14.7 % clay, 24.5 % silt), a low initial pH (5.7), an initial soil TOC and SOM contents of 24.7 g kg^{-1} and 42.8 g kg^{-1}, respectively. Its gravimetric water content at field capacity (-33 kPa) was measured to be 0.23 g g^{-1} (ISO/NF 11274).

In the farm plot, fall seeded rye and triticale have been grown in rotation since 2005 and have replaced a conifer forest. Local practices are as follows: soil tillage is conducted before sowing each crop, a field roller is used after sowing to ensure light soil compaction for germination.

The field (30 m × 63 m) experiment, performed over a rye growth season (October 2021 – July 2022), was set up in a randomized block design with three treatments: control (no liming product amendment), marine $CaCO_3$ and synthetic $CaCO_3$ application both at the neutralizing rate of 2939 neutralising value per ha as defined with the Rémy and Marin-Laflèche (1974) formula to reach a soil pH of 6.8 (Hénault et al., 2019). There were three replicate plots per treatment with each subplot measuring 12 m × 6 m (Figure 1). The liming products were applied in October 2021 just after sowing the rye. Nitrogen fertiliser (50 kg N ha^{-1}), composed with 33.5 % of ammonium nitrate, was applied on soil surface in March 2022 for all treatments.

A weather station (ET 106 model, Campbell) was installed on the farm plot in November 2021 (one month after liming amendments), equipped with a rain gauge and a temperature probe. The soil bulk density (BD) was determined from field measurements on the harvesting day using the cylinder method, (Hao et al., 2008). It ranged between 1.1 g cm^{-3} and 1.2 g cm^{-3} among subplots.

Gas flux measurement

Carbon dioxide and N_2O fluxes were determined using static closed chambers. All data are expressed both in their classical specific units (kg C ha^{-1} d^{-1} or g N ha^{-1} d^{-1} respectively) and specified in CO_2 equivalent, considering the global warming potential with a time horizon of 100 years of each gas (1 for CO_2, 265 for N_2O, Masson-Delmotte et al., 2021), for the purpose of comparison. Three steel frames (0.5 m long × 0.5 m wide × 0.15 m high) were permanently half-inserted into the soil for each subplot (Figure 1) for a total of 27 chambers, 9 per treatment. For the gas measurements, an airtight foamed PVC cover was placed on each of these frames and closed hermetically using 4 spring clamps. The observation period began in October 2021, and the gas samples were taken once weekly (with the exception of few dates during the winter period due to poor weather or lack of human resources). Four gas samples were collected from the chamber headspace using 12 mL syringes at fixed intervals of 45 min after the chamber was closed (T_0 being taken just after closure). Daily CO_2 and N_2O fluxes were determined according to the measurement slope of the linear increase or decrease in gas concentration during the period when the chamber was closed (Zheng et al., 2008). A gas chromatograph (GC) with a thermal conductivity detector (Agilent 990 microGC) coupled with an autosampler (SRA Instruments) and a GC with an electron capture detector (Trace 1310 series GC, Thermo Fisher Scientific) coupled with a TriPlus™ autosampler were used to determine the CO_2 and N_2O concentration, respectively. The minimum detection limits were defined at 0.2 g N-N_2O ha^{-1} d^{-1} and 1000 g C-CO_2 ha^{-1} d^{-1} for the N_2O and CO_2 fluxes, respectively.

As long as the height of the vegetation remained below 5cm, the measurements were carried out in its presence. The vegetation was then cut at the root collar and removed from the chamber before each gas sampling, allowing us to not consider the plant respiration in our gas measurements.

Weekly soil sampling and analyses

Soil samples (0–20 cm soil depth) were collected from each subplot (in the dedicated area as shown in Figure 1) when the flux measurements were performed. They were sieved at 5 mm and placed in Ziploc® plastic bags before almost immediate laboratory analysis. One part was used to determine the soil gravimetric water content (GWC) by drying at 105 °C (24 h). The mineral N (NH_4^+-N and NO_3^--N) contents of soil were extracted in a 10 g subsample with 0.5 M K_2SO_4 and analysed by using the spectrophotometric method (Baethgen and Alley, 1989 ; Cataldo et al., 1975). The detection limit was 0.01 mg N kg^{-1} soil. Another 10 g subsample of soil was shaken for 1h with 50 ml of DI water to measure the soil pH (NF ISO 10390 Mai 2005 / X31-117).

GWC was used to calculate water-filled pore space (WFPS) with equation 4 (Linn and Doran, 1984), with PD; the mineral particle density was estimated at 2.65 g cm^{-3}

$$WFPS = \frac{GWC \times BD}{1 - {BD}/{PD}} \quad \#(4)$$

Soil and plant sampling and analyses on harvesting day (22 July 2022)

In addition to the above soil analyses, the SOC pool was assessed on the harvesting day. Three soil sample replicates per subplot were sent to the SADEF laboratory to identify, with an elementary analyser, the TOC content (TOC_{EA}, g kg^{-1}) and the SOM content (g kg^{-1}). Three other soil sample replicates per subplot were dried at 45°C for 72h and ground (20 min at 30 hertz) before being sent to the ISTO laboratory for Rock-Eval® (RE) thermal analyses. The objectives of this RE pyrolysis were to provide insights into SOC bulk chemistry using RE pyrolysis parameters linked to SOC elemental composition (i.e. hydrogen index, HI and oxygen indices OI_{RE6}, Baudin et al., 2015). Finally, dissolved organic and inorganic carbon (DOC and DIC) were measured by an Elemental TOC analyser after distilled water extraction (WEOC method, Guigue et al., 2014).

194 A 1 m^2 rye biomass was harvested from each subplot (Figure 1) using an electric pruner
195 cutting at 15 cm above the soil. The rye ears were separated from the stalks manually and
196 placed in craft paper bags to be weighed after being placed for 48 hours in an oven at 85°C.
197 The ears were threshed and the weight of the kernels was measured. Finally, the following
198 yield components were measured: total biomass (g m^{-2}), kernel yield (g m^{-2}), thousand-kernel-
199 weight (TKW, g) and specific weight (SW, kg hl^{-1}).

200 The yield-scaled GHG_x emissions (kg GHGx Mg^{-1}) were determined (Equation 5), x
201 being either N_2O, CO_2 or both.

202 $$\text{Yield} - \text{scaled } GHGx \text{ emissions} = \frac{\text{cumulative annual GHGx emissions}}{\text{annual dry rye production}} \#(5)$$

203

204 *Statistical analyses*

205 The statistical analyses were conducted using R software version 4.1.2 (R core team,
206 2018). The normality of data distribution was ascertained visually with a QQ plot and the data
207 were log-transformed when needed. If this transformation proved insufficient, appropriate non-
208 parametric tests were then applied on the response variables, depending on the number of
209 factors involved (e.g., Kruskal-Wallis test or a two-way repeated measures ANOVA with a
210 rank transformation on the variable; Higgins et al., 1990). Factorial mixed ANOVA analyses
211 was conducted for the CO_2, N_2O and CO_2 + N_2O emissions with "liming treatment", "block"
212 as between-group variables and "time" as repeated-measures variables (Field et al., 2012).
213 Factorial independent ANOVA analyses were used for the WFPS, pH and soil N concentrations
214 with "liming treatment", "block" and "time" as between-group variables. One-way
215 independent ANOVA analyses were used to compare rye yield, yield-scaled GHG emissions,
216 soil base saturation percentage, and the inorganic and organic soil carbon indices of the
217 different liming treatments (Control, MC and SC). If a significant difference was found at a p
218 value < 0.05, a Tukey's HSD test was performed to determine the significance of differences

between treatments. In the case of a difference in the confidence intervals of the means between groups, despite undetected differences by ANOVA, t-tests were used for pairwise comparisons (Hsu, 1996; Midway et al., 2020).

Results

Evolution of environmental and soil factors over time

Average air temperature was 8.7°C with a maximum of 27°C observed on 18th of June 2022 (Figure 2a). Temperatures under 10°C were observed until the end of April 2022. A total of 508 mm of rainfall was recorded on the farm plot with precipitations every month, except in July 2022 (Figure 2a).

WFPS ranged from 18.8% to 73% over the experimental period (Figure 2b). This equates with a gravimetric water content ranging from 0.11 g water g^{-1} soil to 0.34 g water g^{-1} soil and which remained over field capacity (0.23 g water g^{-1} soil) until May 2022 for all the treatments. The average WFPSs were 43.4%, 45.8% and 48% for the control, SC and MC, respectively. Limed treatment significantly increased WFPS compared to the control while no significant difference was observed between the MC and SC treatments (Supplementary Table 2).

The soil pH responded very quickly to the application of liming products (MC and SC) and reached the targeted pH of 6.8 during the first month following the application (Figure 2c). Although soil pH exhibited periodic increases and decreases, soil pHs for both liming treatments were significantly higher (Supplementary Table 2) than the soil pH of the control throughout the entire experimental period (Figure 2c). For the control, soil pH fluctuated between 5.48 and 6.36, between 6.64 and 7.88 for the SC treatment, and between 6.45 and 7.78 for the MC treatment.

In general, soil mineral N contents were low in the soil over time. Ammonium-N contents varied from 0.1 to 29.2 mg N kg^{-1} soil (Figure 2d), with significant difference detected between treatments (Supplementary Table 2). Over the entire experimental period, the mean soil NH_4^+-N concentrations were 7.1, 6.4, and 6.1 mg N kg^{-1} soil for the control, SC, and MC treatments, respectively. Nitrate-N contents varied from 0.1 to 19.4 mg N kg^{-1} soil through time (Figure 2e). The average NO_3^--N contents across the rye growth season in the control, SC, and MC treatments were 3.8, 3.0 and 3.0 mg N kg^{-1} soil, respectively and significant differences were temporarily detected between the treatments (Supplementary Table 2), i.e., following N mineral fertilisation.

The percentage of soil base saturation for cations at the end of the experimental period can be found in the Table 1. Liming treatments significantly increased the Ca^{2+} concentration and decreased the H^+ concentration compared to the control. The concentration of K^+ and Mg^{2+} in the soil remained unchanged by the liming treatment.

Evolution of greenhouse gas (CO_2 and N_2O) emissions

Daily N_2O emission fluxes ranged from 0.2 to 18.0 g N-N_2O ha^{-1} d^{-1}, i.e. 0.1 to 7.4 kg CO_2eq and daily CO_2 emissions fluxes ranged from 10 to 184 kg CO_2eq ha^{-1} d^{-1} (Figure 3). Taking account of the specific gas global warming potential, N_2O represented less than 5% of (N_2O + CO_2) emission for 75% of the data, with a median value of this ratio being 1.6%.

The highest N_2O fluxes occurred in autumn, at the beginning of the experimental period, and during summer with peaks between 10 and 20 g N-N_2O emission, while N_2O fluxes were lower than 5 g N-N_2O ha^{-1} d^{-1} from January 2022 to mid-May 2022. No N_2O emission peaks were observed following the application of fertiliser for all three treatments, but 3 peaks were observed following the highest WFPS from Mid-May until August 2022 (Figure 3a). Time significantly affected daily N_2O emissions (Supplementary Table 2). Over the experimental

period, the total N_2O emissions were observed in the order MC > SC > control with a significant difference between treatments. On average, cumulative N_2O emissions were 0.74, 0.92 and 0.89 kg N ha^{-1} for the control, MC and SC treatments, respectively (Table 2). N_2O emissions presented no correlation with temperature or soil moisture for any of the treatments (Figure 4 & 5).

CO_2 fluxes were lower during the winter period and started to increase in March 2022 to reach their maximum during the summer period for all the treatments (Figure 3b). Four peaks can be observed on the 28th April, 24th May, 9th and 23rd June 2022. Time significantly affected daily CO_2 fluxes (Supplementary Table 2). Temperature had a significant positive effect on daily soil CO_2 emissions throughout the experimental period, irrespective of liming treatments. Mean daily CO_2 emissions was negatively correlated to soil WFPS during the study (Figure 4 & 5). Liming did not affect the relationship between daily CO_2 emissions and abiotic factors across flux measurement dates. Liming treatment influenced daily CO_2 fluxes over the rye growing season (Figure 3b), with significantly lower CO_2 fluxes for both liming treatments compared to the control (Supplementary Table 2). There was no significant difference in CO_2 emission between either liming treatment. For the control treatment, the average daily CO_2 flux was 19.7 kg C ha^{-1} d^{-1} while it was 12.2 and 11.6 kg C ha^{-1} d^{-1}, respectively for the MC and SC treatments. The CO_2 abatement caused by liming applications could be estimated at 3.74 and 3.94 mg C kg^{-1} soil d^{-1} for the MC and SC treatments, respectively. Between liming application and harvesting, 273 days had passed, thus losses of 1.02 and 1.08 g C kg^{-1} soil were avoided by MC and SC, respectively.

This treatment effect was passed on to the overall fluxes (CO_2 + N_2O, Figure 3c), with significantly lower CO_2 equivalent emissions for both liming treatments compared to the control with on average, over time, 73.6, 46.4 and 44.1 kg CO_2 eq ha^{-1} d^{-1} for the control, MC and SC, respectively, representing abatements of 37% and 40%.

293

294 *Rye yield and yield-scaled emissions*

295 Rye yields for the treatments are shown in Table 2. There was a trend of increase in rye
296 yield with higher yields for both liming treatments compared to the yield of the control.
297 However, only the total kernel yield for the MC treatment was proved to be significantly higher
298 than the control. Also not significant, total kernel yield and specific weight were also observed
299 to be higher for both liming treatments compared to the control (Table 2).

300 There was no significant difference between treatments for the yield-scaled N_2O
301 emissions but significant difference after liming application for the yield-scaled CO_2 emissions
302 and yield-scaled GHG balance ($CO_2 + N_2O$) (Table 2). Totals of $8.9e10^{-2}$, $9.4e10^{-2}$ and $9.3e10^{-2}$
303 kg N Mg^{-1} were emitted from the control, MC and SC treatments, respectively.

304

305 *The C pool remaining in the soil after harvesting*

306 Due to the very high difference in CO_2 fluxes observed between the control and the
307 limed treatments, we investigated the remaining C pool at harvest.

308 Total organic carbon (TOC_{RE} than TOC_{EA}) was higher, but not significantly, for the
309 control treatment compared to both liming treatments (Table 3). Likewise, SOM was higher,
310 but not significantly, for the control treatment with 46.2 g kg^{-1}, compared to both liming
311 treatments, i.e., 42.2 and 42.3 g kg^{-1} for MC and SC, respectively (Table 3).

312 The quantities of DOC and DIC remaining in the soil after harvesting were significantly
313 higher for both liming treatments (Table 3) compared to the control.

314 Results for the two parameters associated with SOC bulk chemistry (HI and OI_{RE6})
315 suggested an increasing liming effect (Table 3) on both parameters. The MC treatment was
316 characterised by a significantly higher HI whereas the HI value of the SC treatment (198.4 mg
317 HC g^{-1} TOC_{RE}) did not show a significant difference with the control treatment (184 mg HC

g^{-1} TOC_{RE}). Likewise, for the OI_{RE6} parameters, the relatively large standard errors did not lead to a significant difference between treatments despite increased average values for the MC and SC treatments compared to the control (Table 3). Placed in the pseudo-van Krevelen diagram (Figure 6), these indicators suggest a slight change in the composition of the SOC after the application of liming products.

Discussion

Studying the liming impact on acid soil respiration in the field is critical for predicting the benefits of this agricultural practice on climate regulation, the carbon source-sink relationships, and has practical implications for farmers (Wang et al., 2021). After just one year of experimental data, the results already showed a clear mitigation of CO_2 emissions by liming treatments with an average reduction in greenhouse gas emissions (CO_2 + N_2O) of more than 35%, thereby reasserting the agronomic value of liming products.

The application of liming tends to increase plant productivity

The liming of acid soil and the associated increase in soil pH (on average 1.3 pH units for MC and 1.1 pH unit for SC, Figure 2c) stimulated both rye and kernel yields, without however being significant. The yield obtained after liming (Table 2) was identical to the national average despite the application of a lower amount of fertilizer (Agreste Conjuncture, 2022). These increases in yields are probably linked to liming-induced increases in the availability and mobility of plant nutrients (Holland et al., 2019). In this study, the $CaCO_3$ products used led, unsurprisingly, to a higher Ca^{2+} saturation rate of the clay-silt complex for the MC and SC.

The application of liming decreases soil CO_2 emissions and changes SOC bulk chemistry

343 Rates of soil CO_2 emissions recorded in the present study in control plots were within
344 the range of soil CO_2 emissions reported elsewhere in the field, e.g., Cho et al. (2019) measured
345 CO_2 fluxes between 5 and 70 kg C ha^{-1} d^{-1} from a loamy soil in a South Korean plot over two
346 years (2015 and 2016) after liming treatments. From the results obtained by meta-analysis
347 (Wang et al., 2021), an increase in CO_2 emissions after liming application was expected via
348 $CaCO_3$ dissolution with an increase in soil pH and hence soil biological activities and SOC
349 mineralisation (Biasi et al., 2008). However, this hypothesis was not supported by our results.
350 Despite a significant increase in soil pH in both liming plots during the experiment, a reduction
351 of 3.74 and 3.94 mg C kg^{-1} d^{-1} was observed for the MC and SC treatments, respectively. This
352 result suggests that liming had a negative priming effect on SOC mineralisation despite a
353 decreasing trend of SOC in the liming treatments compared to the control (Table 3).
354 Many of the mechanisms controlling SOC stability, making it inaccessible to
355 decomposers and hence preventing mineralisation, have been identified in the past. The
356 stabilisation and maintenance of SOC in mineral soil horizons, has predominantly been thought
357 to be driven by specific ecosystem properties including, among others, interactions between
358 SOC and cations or minerals (Rowley et al., 2018). Previous research in Ca-rich field
359 environments has highlighted a positive correlation between exchangeable Ca^{2+} and SOC
360 concentrations (Clough and Skjemstad, 2000; Bertrand et al., 2007). An increase of the soil
361 concentration in exchangeable Ca^{2+} after liming application will lead to a potential increase of
362 SOC stabilisation (Paradelo et al., 2015) and hence lower CO_2 emissions. Moreover, changes
363 in soil pH initially increase SOC solubility via either deprotonation or desorption reactions
364 (Andersson and Nilsson, 2001) and may stabilise SOC via Ca^{2+} bridging, leading to less
365 leaching and C mineralisation (Rowley et al., 2018). The higher DOC concentrations in the
366 liming treatments supported this hypothesis. Despite a majority of articles showing positive
367 liming effects on CO_2 emissions (Kunhikrishnan et al., 2016), Grover et al. (2017) also

368 observed a decrease in CO_2 emissions after liming and also hypothesised a stabilising effect of
369 Ca^{2+}, emphasising the importance of the initial soil clay concentration.

370 In addition, previous studies using Rock-Eval® analysis have established that the HI
371 and OI_{RE6} indices correlate well with atomic H/C and O/C ratios, respectively, and that the
372 HI:OI_{RE6} plot can be comparable to a classic van Krevelen diagram (Vandenbroucke and
373 Largeau, 2007). Using the example given in Saenger et al. (2013), such HI and OI_{RE6} values
374 (Figure 6) would correspond preferentially to fulvic acids. These soil organic molecules
375 constitute, with humic acid and humic substances, a complex mixture of many different acids
376 extremely resistant to biodegradation (Collado et al., 2018). It is therefore possible that the
377 chemical composition of our SOC was affected by the addition of the liming product, as shown
378 in Figure 6, and tended towards a more stable form, which would also lead to a reduction in
379 CO_2 emissions.
380

381 *Temporal variation in CO_2 emissions and linkages with soil temperature*

382 The rate of soil CO_2 emissions was not only dependent on the liming treatments but
383 also showed considerable temporal variation in all three treatments. Soil respiration is known
384 to vary temporally and spatially, often in parallel with abiotic factors such as temperature and
385 water availability (Raich et al., 2002). The temperature was a stronger predictor of soil CO_2
386 emissions than soil moisture on our 29 dates of flux measurements. Due to the temperature
387 dependence of the biochemical processes and enzyme activities associated with soil respiration,
388 this outcome was expected (Chen et al., 2014; Lochon et al., 2019).

389 However, the temperature sensitivity of soil respiration is known to be affected by
390 microbial communities (Karhu et al., 2014) and plant biomass via changes in assimilate supply
391 (Bahn et al., 2008). Contrary to expectations, liming did not change the relationship between
392 CO_2 emissions and soil temperature or moisture despite the liming effect on plant biomass

observed in the present study. The present study diverges from prior research conducted on the topic of grazing and grassland restoration practices which indicated that management practices altered the susceptibility of soil CO_2 emissions to abiotic drivers (Xue and Tang, 2018) but are similar to the observations of Lochon et al. (2019).

Global GHG avoidance obtained by liming application

As N_2O emissions are also known to be affected by liming products, we also measured them in the field. Soil N_2O flux averages measured for all the treatments remained low throughout the experiment (< 18 g N ha^{-1} d^{-1}; Figure 3a) and in this context the application of liming products did not reduce them. On the contrary, significantly higher fluxes for the liming treatments were observed in December 2021 and for the summer peaks (Figure 3a). For these dates, we assume that the N_2O reductase was fully functional as the pH was above 6.8 for the limed treatments (Ouerghi et al., 2023). Different hypotheses can therefore be formulated to explain these results: (i) although N_2O reductase was functional in the limed soil, it was not active due to the aerobiosis conditions in the soil (WFPS < 0.62, Grundmann & Rolston, 1987); (ii) the N_2O emissions were caused not by the denitrification process but by another process enhanced by liming, probably nitrification (Nadeem et al. 2020).

Holtan-Hartwig et al. (2002) showed that the temperature response of N_2O reduction could be fitted to an Arrhenius function in the range 5–20 °C and that a very low temperature (<5°C) may have a particularly severe effect on the N_2O reduction process. At the beginning of December 2021, temperatures in the field were below 5°C and were potentially unfavourable for N_2O reduction. Wu et al. (2022) also found that the mitigation effect of liming on N_2O emissions can mainly be seen when labile C is highly available in soils. However, the C in our soil was considered extremely resistant to biodegradation. Therefore, these abiotic conditions

(C availability and temperature) could reflect a blockage of N_2O reductase functionality despite a favourable pH.

In addition, during the summer period, NO_3^- content was low and the WFPS under 60%, known to be the threshold for the diffusion of O_2 in the soil atmosphere and consequently the limit between aerobic and anaerobic processes (Davidson, 1993). These conditions were not suitable for the denitrification process. The hypothesis that the N_2O emitting process was nitrification was then suggested. The liming products could stimulate nitrification-driven N_2O production (Nadeem et al., 2020), which would explain our observations. However, it is noteworthy that despite higher N_2O emissions, the GHG balance in our system was reduced in both liming treatments compared to the control. Additional work is now needed to determine whether the findings obtained here for a rye cropping system and the specific initial soil condition can be generalised for different soil types and N land-use intensities as a growing number of studies have suggested that N fertilization and liming may interact (Poozesh et al., 2010; Lochon et al., 2018). The results relating to the GHG balance showed that future studies should also take into consideration not only soil CO_2 and N_2O emissions but also those of CH_4 to more accurately assess the net effect of liming on the global warming balance in the field. Soil pH is one of several factors controlling CH_4 production in soils and increases CH_4 oxidation rates have been observed after increasing soil pH of acid soils (Abushammala et al., 2014).

Conclusion

In the current context of climate emergency, we observed during a one-site and one-year *in situ* experiment, that liming can strongly decrease CO_2 and GHG emissions from soil, with slightly improving grain yield. Probably liming helps SOC stabilisation, through Ca^{2+} effect. More research is still needed to quantify the loss of CO_2 resulting from liming

application through isotope labelling and to precise mechanisms involved in soil CO_2 emission mitigation. Our study should also be extended over time and to different soil types and different N land-use intensities. Nevertheless, these results strongly suggest that liming need to be consider as a potential lever for carbon storage and that IPCC principles estimating an increase of CO_2 emissions linked to the C added by lime materials would need to be re-examined in the future.

Conflicts of Interest

The authors declare no conflicts of interest.

Acknowledgements

The authors gratefully acknowledge funding for the *NatAdGES* project from the "Investissement d'Avenir" program, ISITE-BFC project (contract ANR-15-IDEX-0003), the European Regional Development Fund (FEDER), the public investment bank (BPI France) and CMI-Roullier. They sincerely thank the steering committee of *NatAdGES* for the useful discussions. The authors also wish to express their gratitude to the farmer that has welcome them, to the staff of the GISMO platform (Biogéosciences, UMR 6282 CNRS Université de Bourgogne) and of the ISTO Institute for the technical assistance.

References

Abushammala, M., Basri, N., Irwan, D., Younes, M., 2014. Methane Oxidation in Landfill Cover Soils: A Review. Asian Journal of Atmospheric Environment 8. doi:10.5572/ajae.2014.8.1.001

Andersson, S., Nilsson, S.I., 2001. Influence of pH and temperature on microbial activity, substrate availability of soil-solution bacteria and leaching of dissolved organic carbon in a mor humus. Soil Biology and Biochemistry 33, 1181–1191. doi:10.1016/S0038-0717(01)00022-0

Bahn, M., Rodeghiero, M., Anderson-Dunn, M., Dore, S., Gimeno, C., Drösler, M., Williams, M., Ammann, C., Berninger, F., Flechard, C., Jones, S., Balzarolo, M., Kumar, S., Newesely, C., Priwitzer, T., Raschi, A., Siegwolf, R., Susiluoto, S., Tenhunen, J., Wohlfahrt, G., Cernusca, A., 2008. Soil Respiration in European

Grasslands in Relation to Climate and Assimilate Supply. Ecosystems (New York, N.Y.) 11, 1352–67. doi:10.1007/s10021-008-9198-0

Baudin, F., Disnar, J.-R., Aboussou, A., Savignac, F., 2015. Guidelines for Rock–Eval analysis of recent marine sediments. Organic Geochemistry 86, 71–80. doi:10.1016/j.orggeochem.2015.06.009

Bertrand, I., Delfosse, O., Mary, B., 2007. Carbon and nitrogen mineralization in acidic, limed and calcareous agricultural soils: Apparent and actual effects. Soil Biology and Biochemistry 39, 276–288. doi:10.1016/j.soilbio.2006.07.016

Biasi, C., Lind, S.E., Pekkarinen, N.M., Huttunen, J.T., Shurpali, N.J., Hyvönen, N.P., Repo, M.E., Martikainen, P.J., 2008. Direct experimental evidence for the contribution of lime to CO_2 release from managed peat soil. Soil Biology and Biochemistry 40, 2660–2669. doi:10.1016/j.soilbio.2008.07.011

Blum, Winfried.E.H., Schad, P., Nortcliff, S., 2017. Essentials of Soil Science. CSIRO Publishing.

Chen, S., Zou, J., Hu, Z., Chen, H., Lu, Y., 2014. Global annual soil respiration in relation to climate, soil properties and vegetation characteristics: Summary of available data. Agricultural and Forest Meteorology 198–199, 335–346. doi:10.1016/j.agrformet.2014.08.020

Cho, S.R., Jeong, S.T., Kim, G.Y., Lee, J.G., Kim, P.J., Kim, G.W., 2019. Evaluation of the carbon dioxide (CO_2) emission factor from lime applied in temperate upland soil. Geoderma 337, 742–748. doi:10.1016/j.geoderma.2018.10.007

Clough, A., Skjemstad, J.O., 2000. Physical and chemical protection of soil organic carbon in three agricultural soils with different contents of calcium carbonate. Soil Research 38, 1005–1016. doi:10.1071/sr99102

Collado, S., Oulego, P., Suárez-Iglesias, O., Díaz, M., 2018. Biodegradation of dissolved humic substances by fungi. Applied Microbiology and Biotechnology 102, 3497–3511. doi:10.1007/s00253-018-8851-6

Davidson, E.A., 1993. Soil Water Content and the Ratio of Nitrous Oxide to Nitric Oxide Emitted from Soil, in: Oremland, R.S. (Ed.), Biogeochemistry of Global Change: Radiatively Active Trace Gases Selected Papers from the Tenth International Symposium on Environmental Biogeochemistry, San Francisco, August 19–24, 1991. Springer US, Boston, MA, pp. 369–386. doi:10.1007/978-1-4615-2812-8_20

Dumale Jr., W.A., Miyazaki, T., Hirai, K., Nishimura, T., 2011. SOC Turnover and Lime-CO_2 Evolution during Liming of an Acid Andisol and Ultisol. Open Journal of Soil Science 01, 49–53. doi:10.4236/ojss.2011.12007

Field, A., Miles, J., Field, Z., 2012. Discovering statstics using R, SAGE Publications Ltd. ed. SAGE Publications Ltd.

Fornara, D.A., Steinbeiss, S., Mcnamara, N.P., Gleixner, G., Oakley, S., Poulton, P.R., Macdonald, A.J., Bardgett, R.D., 2011. Increases in soil organic carbon sequestration can reduce the global warming potential of long-term liming to permanent grassland. Global Change Biology 17, 1925–1934. doi:10.1111/j.1365-2486.2010.02328.x

Fuentes, J.P., Bezdicek, D.F., Flury, M., Albrecht, S., Smith, J.L., 2006. Microbial activity affected by lime in a long-term no-till soil. Soil and Tillage Research 88, 123–131. doi:10.1016/j.still.2005.05.001

Grover, S.P., Butterly, C.R., Wang, X., Gleeson, D.B., Macdonald, L.M., Tang, C., 2021. Liming and priming: the long-term impact of pH amelioration on mineralisation may negate carbon sequestration gains. Soil security 3. doi:10.1016/j.soisec.2021.100007

Grover, S.P., Butterly, C.R., Wang, X., Tang, C., 2017. The short-term effects of liming on organic carbon mineralisation in two acidic soils as affected by different rates and

application depths of lime. Biology and Fertility of Soils 53, 431–443. doi:10.1007/s00374-017-1196-y

Grundmann, G.L., Rolston D.E., 1987 A water function approximation to degree of anaerobiosis associated with denitrification. Soil Science 144, 437–441. doi: 10.1097/00010694-198712000-00008

Guigue, J., Mathieu, O., Lévêque, J., Mounier, S., Laffont, R., Maron, P.A., Navarro, N., Chateau, C., Amiotte-Suchet, P., Lucas, Y., 2014. A comparison of extraction procedures for water-extractable organic matter in soils. European Journal of Soil Science 65, 520–530. doi:10.1111/ejss.12156

Hamilton, S.K., Kurzman, A.L., Arango, C., Jin, L., Robertson, G.P., 2007. Evidence for carbon sequestration by agricultural liming. Global Biogeochemical Cycles 21. doi:10.1029/2006GB002738

Hao, X., Bal, B.C., Culley, J.L.B., Carter, M.R., Parkin, G.W., 2008. Soil density and porosity. Soil Sampling and Methods of Analysis. 743–760

Hénault, C., Bourennane, H., Ayzac, A., Ratié, C., Saby, N.P.A., Cohan, J.-P., Eglin, T., Gall, C.L., 2019. Management of soil pH promotes nitrous oxide reduction and thus mitigates soil emissions of this greenhouse gas. Scientific Reports 9, 20182. doi:10.1038/s41598-019-56694-3

Holland, J.E., Bennett, A.E., Newton, A.C., White, P.J., McKenzie, B.M., George, T.S., Pakeman, R.J., Bailey, J.S., Fornara, D.A., Hayes, R.C., 2018. Liming impacts on soils, crops and biodiversity in the UK: A review. Science of The Total Environment 610–611, 316–332. doi:10.1016/j.scitotenv.2017.08.020

Holland, J.E., White, P.J., Glendining, M.J., Goulding, K.W.T., McGrath, S.P., 2019. Yield responses of arable crops to liming – An evaluation of relationships between yields

546 and soil pH from a long-term liming experiment. European Journal of Agronomy 105,
547 176–188. doi:10.1016/j.eja.2019.02.016
548 Holtan-Hartwig, L., Dörsch, P., Bakken, L.R., 2002. Low temperature control of soil
549 denitrifying communities: kinetics of N_2O production and reduction. Soil Biology and
550 Biochemistry 34, 1797–1806. doi:10.1016/S0038-0717(02)00169-4
551 Hsu, J., 1996. Multiple Comparisons: Theory and Methods. Chapman and Hall/CRC, New
552 York. doi:10.1201/b15074
553 Jones, C.M., Graf, D.R., Bru, D., Philippot, L., Hallin, S., 2013. The unaccounted yet
554 abundant nitrous oxide-reducing microbial community: a potential nitrous oxide sink.
555 The ISME Journal 7, 417–426. doi:10.1038/ismej.2012.125
556 Karhu, K., Auffret, M.D., Dungait, J.A.J., Hopkins, D.W., Prosser, J.I., Singh, B.K., Subke,
557 J.-A., Wookey, P.A., Ågren, G.I., Sebastià, M.-T., Gouriveau, F., Bergkvist, G., Meir,
558 P., Nottingham, A.T., Salinas, N., Hartley, I.P., 2014. Temperature sensitivity of soil
559 respiration rates enhanced by microbial community response. Nature 513, 81–84.
560 doi:10.1038/nature13604
561 Kravchenko, A.N., Toosi, E.R., Guber, A.K., Ostrom, N.E., Yu, J., Azeem, K., Rivers, M.L.,
562 Robertson, G.P., 2017. Hotspots of soil N_2O emission enhanced through water
563 absorption by plant residue. Nature Geoscience 10, 496–500. doi:10.1038/ngeo2963
564 Kunhikrishnan, A., Thangarajan, R., Bolan, N.S., Xu, Y., Mandal, S., Gleeson, D.B.,
565 Seshadri, B., Zaman, M., Barton, L., Tang, C., Luo, J., Dalal, R., Ding, W., Kirkham,
566 M.B., Naidu, R., 2016. Functional Relationships of Soil Acidification, Liming, and
567 Greenhouse Gas Flux, in: Advances in Agronomy. Elsevier, pp. 1–71.
568 doi:10.1016/bs.agron.2016.05.001

569 Lochon, I., Carrère, P., Revaillot, S., Bloor, J.M.G., 2018. Interactive effects of liming and
570 nitrogen management on carbon mineralization in grassland soils. Applied Soil
571 Ecology 130, 143–148. doi:10.1016/j.apsoil.2018.06.010
572 Lochon, I., Carrère, P., Yvin, J.-C., Houdusse-Lemenager, D., Bloor, J.M.G., 2019. Impacts
573 of low-level liming on soil respiration and forage production in a fertilized upland
574 grassland in Central France. Science of The Total Environment 697, 134098.
575 doi:10.1016/j.scitotenv.2019.134098
576 Masson-Delmotte, V., Zhai, P., Pirani, A., Connors, S.L., Péan, C., Berger, S., Caud, N.,
577 Chen, Y., Goldfarb, L., Gomis, M.I., Huang, M., Leitzell, K., Lonnoy, E., Matthews,
578 J.B.R., Maycock, T.K., Waterfield, T., Yelekçi, O., Yu, R., Zhou B., 2021 Climate
579 Change 2021: The Physical Science Basis. Contribution of Working Group I to the
580 Sixth Assessment Report of the Intergovernmental Panel on Climate Change.
581 Cambridge University Press, doi: 10.1017/9781009157896
582 Midway, S., Robertson, M., Flinn, S., Kaller, M., 2020. Comparing multiple comparisons:
583 practical guidance for choosing the best multiple comparisons test. PeerJ 8, e10387.
584 doi:10.7717/peerj.10387
585
586 Nadeem, S., Bakken, L.R., Frostegård, Å., Gaby, J.C., Dörsch, P., 2020. Contingent effects of
587 liming on N_2O-emissions driven by autotrophic nitrification. Frontiers in
588 Environmental Science 8. doi:10.3389/fenvs.2020.598513
589 Oades, J.M., 1984. Soil organic matter and structural stability: mechanisms and implications
590 for management. Plant and Soil 76, 319–337. doi:10.1007/BF02205590
591 Ouerghi, I., Rousset, C., Bizouard, F., Brefort, H., Ubertosi, M., Arkoun, M., Hénault, C.,
592 2023. Hysteretic response of N_2O reductase activity to soil pH variations after
593 application of lime to an acidic agricultural soil. Biol Fertil Soils 59, 473–479.
594 doi.org/10.1007/s00374-023-01717-5

595 Paradelo, R., Virto, I., Chenu, C., 2015. Net effect of liming on soil organic carbon stocks: A
596 review. Agriculture, Ecosystems & Environment 202, 98–107.
597 doi:10.1016/j.agee.2015.01.005
598 R Core Team 2018. R: A language and environment for statistical computing. R Foundation
599 for Statistical Computing, Vienna, Austria.URL: https://www.R-project.org/
600 Raich, J.W., Potter, C.S., Bhagawati, D., 2002. Interannual variability in global soil
601 respiration, 1980–94. Global Change Biology 8, 800–812. doi:10.1046/j.1365-
602 2486.2002.00511.x
603 Remy, J.C., Marin-Laflèche, A., 1974 L'analyse de terre : réalisation d'un programme
604 d'interprétation automatique. Annales Agronomiques 25, 607-632.
605 Ritchie, H., Roser, M., Rosado, P., 2020. "CO_2 and Greenhouse Gas Emissions". Published
606 online at OurWorldInData.org. URL: 'https://ourworldindata.org/co2-and-greenhouse-
607 gas-emissions'
608 Rowley, M.C., Grand, S., Verrecchia, É.P., 2018. Calcium-mediated stabilisation of soil
609 organic carbon. Biogeochemistry 137, 27–49. doi:10.1007/s10533-017-0410-1
610 Saenger, A., Cécillon, L., Sebag, D., Brun, J.-J., 2013. Soil organic carbon quantity,
611 chemistry and thermal stability in a mountainous landscape: A Rock–Eval pyrolysis
612 survey. Organic Geochemistry 54, 101–114. doi:10.1016/j.orggeochem.2012.10.008
613 Shaaban, M., Peng, Q., Hu, R., Wu, Y., Lin, S., Zhao, J., 2015. Dolomite application to acidic
614 soils: a promising option for mitigating N_2O emissions. Environmental Science and
615 Pollution Research 22, 19961–19970. doi:10.1007/s11356-015-5238-4
616 Vandenbroucke, M., Largeau, C., 2007. Kerogen origin, evolution and structure. Organic
617 Geochemistry 38, 719–833. doi:10.1016/j.orggeochem.2007.01.001
618 Wang, Y., Yao, Z., Zhan, Y., Zheng, X., Zhou, M., Yan, G., Wang, L., Werner, C.,
619 Butterbach-Bahl, K., 2021. Potential benefits of liming to acid soils on climate change

mitigation and food security. Global Change Biology 27, 2807–2821. doi:10.1111/gcb.15607

West, T.O., McBride, A.C., 2005. The contribution of agricultural lime to carbon dioxide emissions in the United States: dissolution, transport, and net emissions. Agriculture, Ecosystems & Environment 108, 145–154. doi:10.1016/j.agee.2005.01.002

Wu, L., Xiao, Q., Wang, J., Huang, Y., Wu, D., Liu, J., Wang, B., Zhang, H., Xu, M., Zhang, W., 2022. Liming decreases the emission and temperature sensitivity of N_2O following labile carbon addition. Geoderma 425, 116032. doi:10.1016/j.geoderma.2022.116032

Wuddivira, M.N., Camps-Roach, G., 2007. Effects of organic matter and calcium on soil structural stability. European Journal of Soil Science 58, 722–727. doi:10.1111/j.1365-2389.2006.00861.x

Xue, H., Tang, H., 2018. Responses of soil respiration to soil management changes in an agropastoral ecotone in Inner Mongolia, China. Ecology and Evolution 8, 220–230. doi:10.1002/ece3.3659

Zheng, X., Mei, B., Wang, Yinghong, Xie, B., Wang, Yuesi, Dong, H., Xu, H., Chen, G., Cai, Z., Yue, J., Gu, J., Su, F., Zou, J., Zhu, J., 2008. Quantification of N_2O fluxes from soil–plant systems may be biased by the applied gas chromatograph methodology. Plant and Soil 311, 211–234. doi:10.1007/s11104-008-9673-6

References

List of figures and tables:

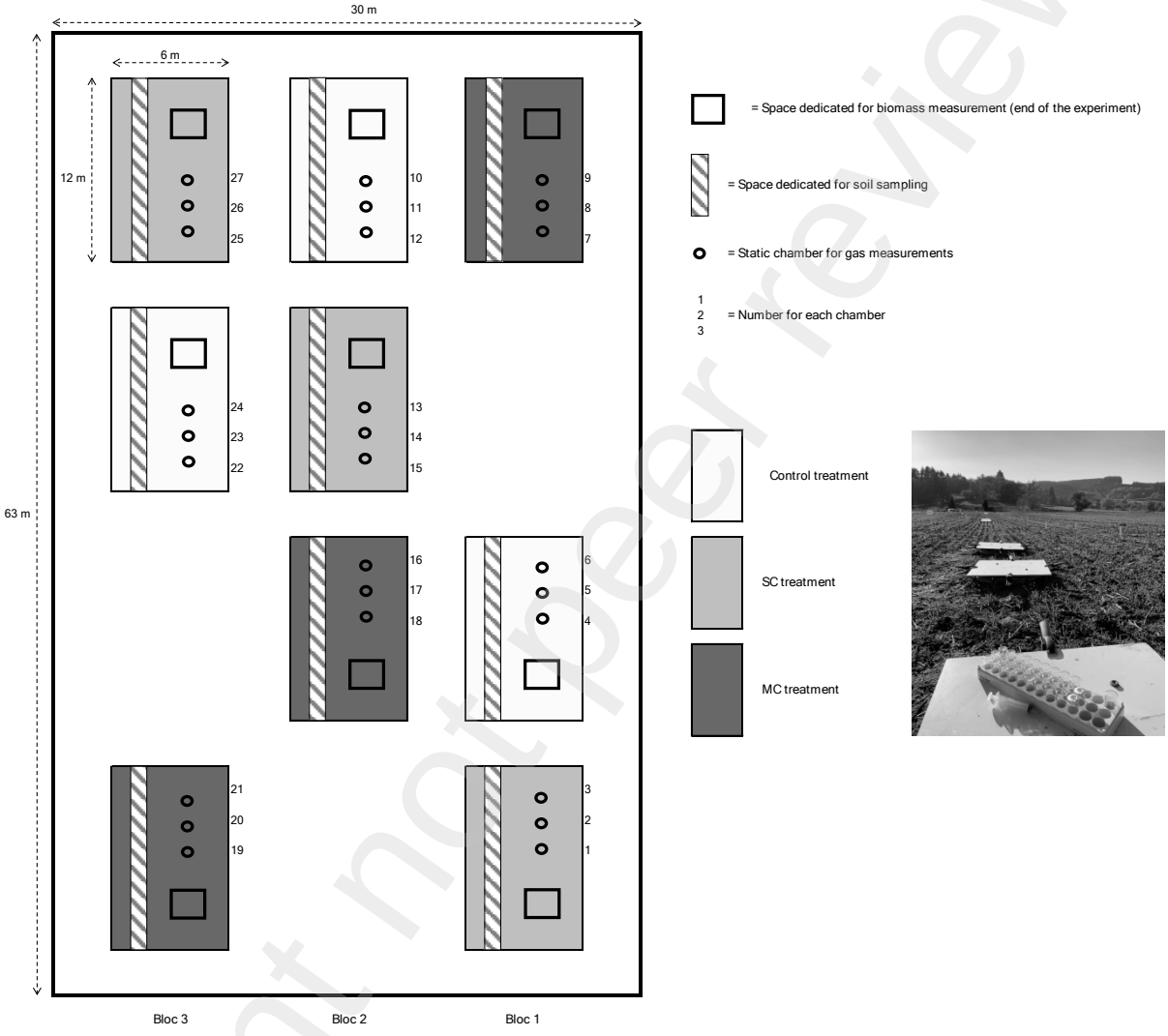

FIGURE 1: Schematic representation of the experimental site.

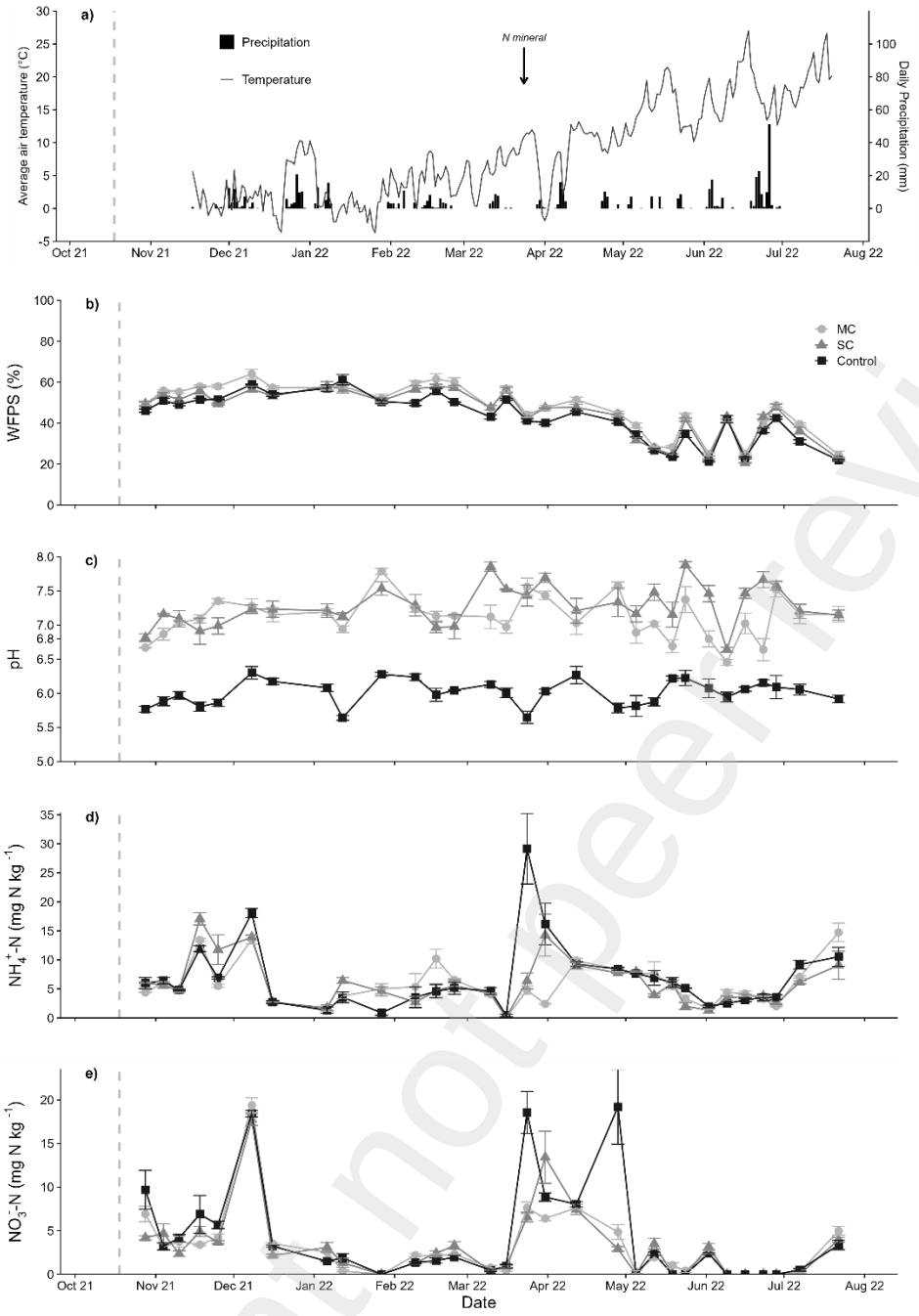

646

647 *FIGURE 2: Experimental climatic conditions (average daily temperature and daily*
648 *precipitation) from the 17th of November 2021 until 22th July 2022 (graphic a). Soil dynamics:*
649 *b) water filled pore space (WFPS), c) pH, d) ammonium-N (NH_4^+-N) and e) nitrate-N (NO_3^--*
650 *N) of the three treatments (control, MC and SC) in the rye field from 28th October 2021 to 22th*
651 *July 2022. Liming products were applied on 19th October 2021, as shown by the horizontal*
652 *dashed line. Mineral N was applied on 24th March 2022, represented by the arrow. Error bars*
653 *= s.e.m. n=3.*

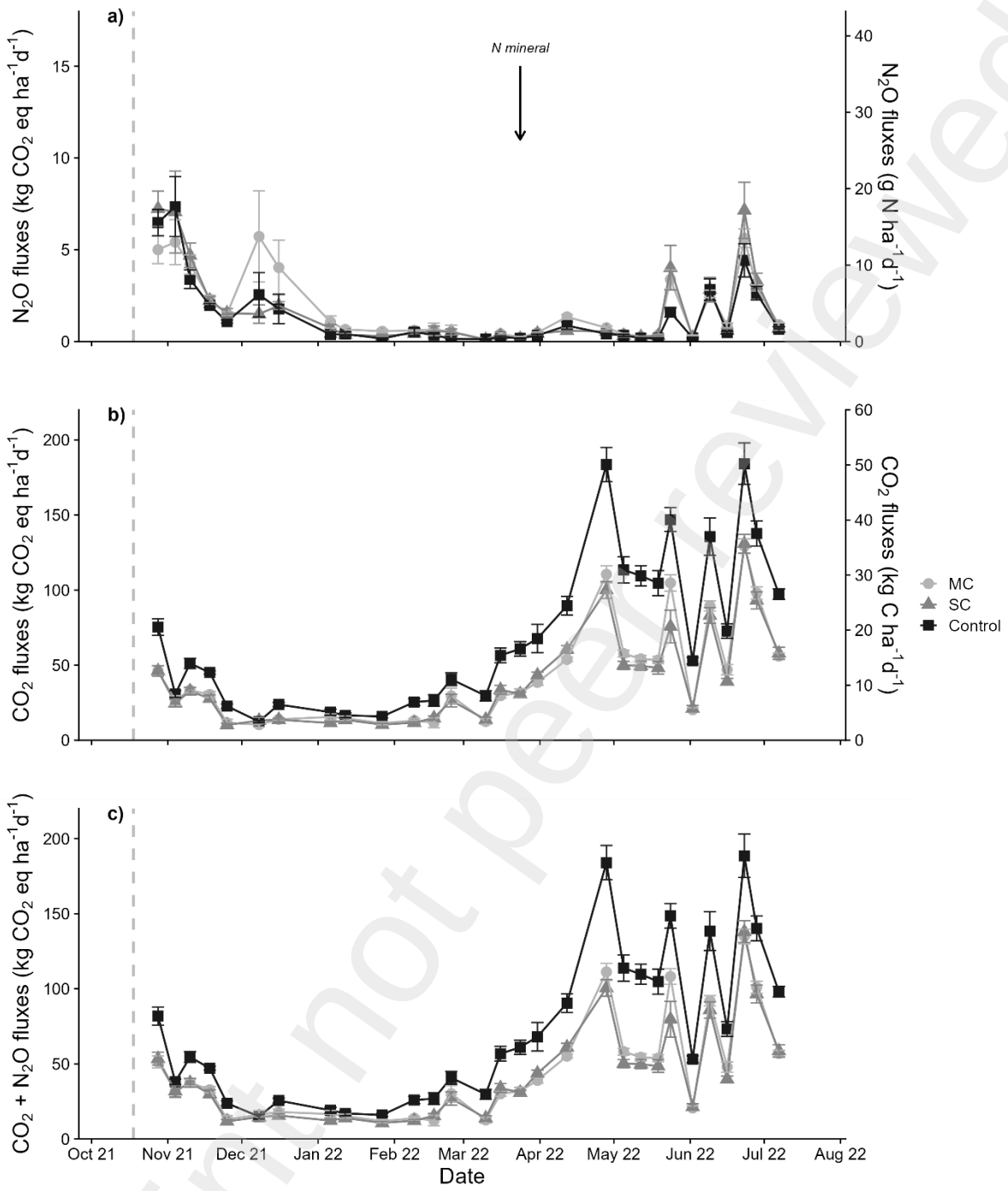

654

655 *FIGURE 3: Dynamics of: a) N_2O emissions, b) CO_2 emissions c) Total (CO_2 + N_2O) emissions*
656 *expressed in CO_2 equivalent and their equivalents in kg C ha^{-1} d^{-1} and g N ha^{-1} d^{-1}, of the three*
657 *treatments (control, MC and SC) in the rye field from 28th October 2021 to 22th July 2022.*
658 *Liming products were applied on 19th October 2021, as shown by the horizontal dashed line.*
659 *N mineral was applied on 24th March 2022 represented by the arrow. Error bars = s.e.m. n=9.*

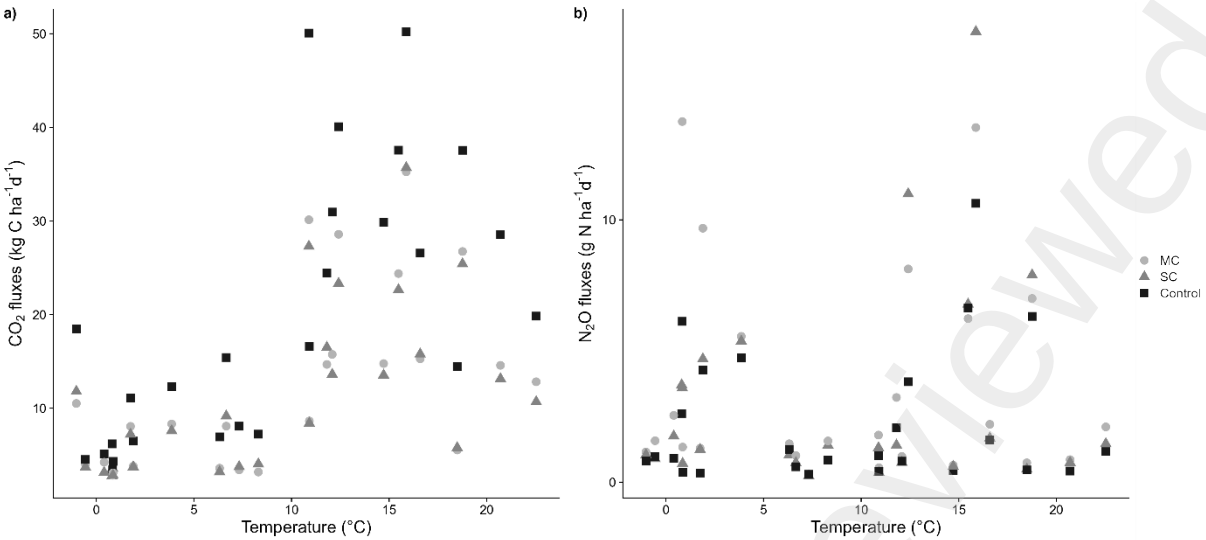

660

661 *FIGURE 4: Relationship between air temperature and a) CO_2 emissions, b) N_2O emissions for*

662 *the three treatments (control, MC and SC).*

663

664

665

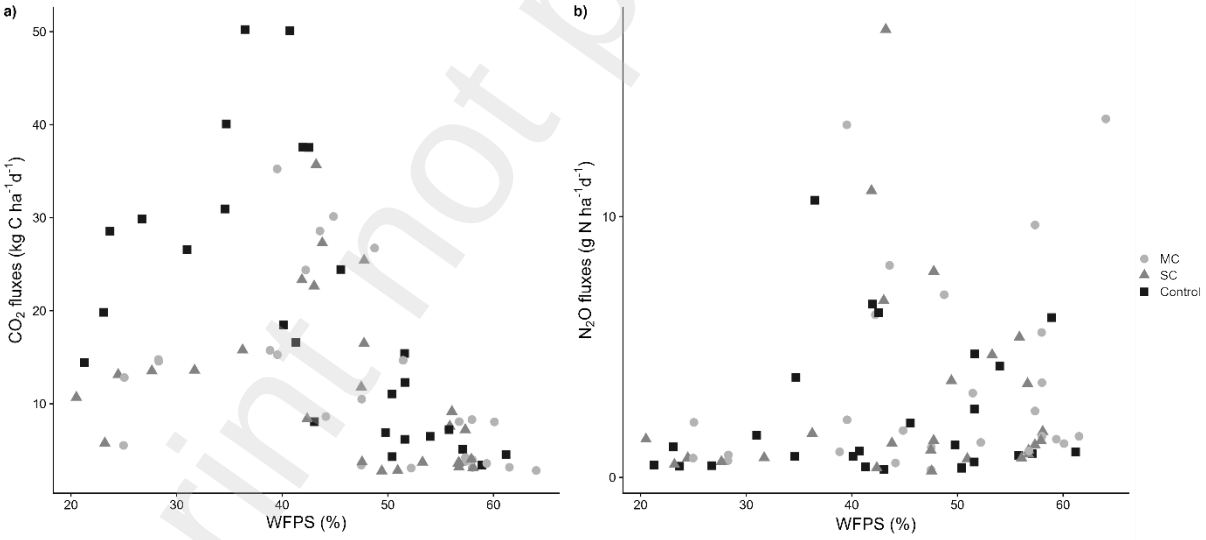

666

667 *FIGURE 5: Relationship between WFPS and a) CO_2 emissions, b) N_2O emissions for the three*

668 *treatments (control, MC and SC).*

669

670

671

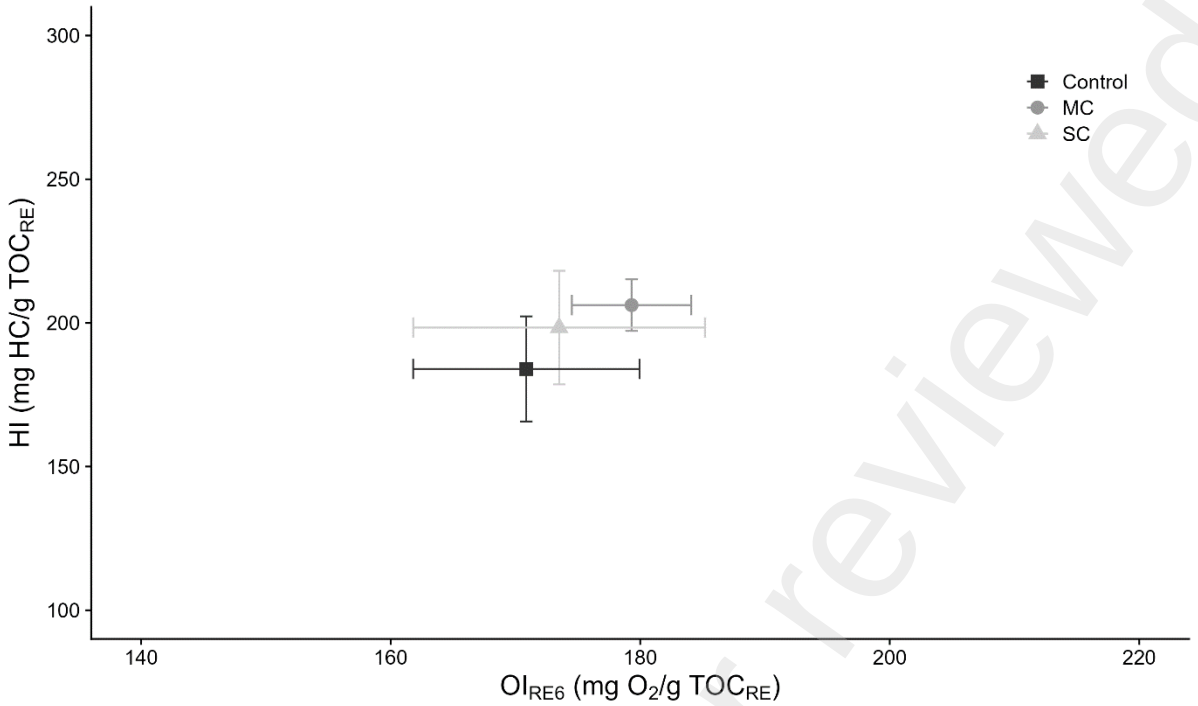

672

673 *FIGURE 6: Position of the average soil samples in the pseudo-van Krevelen diagram (HI vs.*

674 *OI_{RE6}) according to the 3 treatments, , with the hydrogenation index (HI) and the Oxygen Index*

675 *(OI_{RE6}).*

676

677 *Table 1: Average of the soil base saturation percentage (Ca2+, K+ Mg2+ and H+) computed*

678 *for each treatment. Different characters in the same line indicate significance at the 0.05 level*

679 *based on one-way ANOVA. MC and SC are liming treatments.*

Treatment	Ca^{2+}		K^{+}		Mg^{2+}		H^{+}	
	%		%		%		%	
Control	41.0	b	4.5	a	4.1	a	50.0	a
MC	78.7	a	3.6	a	4.1	a	13.0	b
SC	68.8	a	4.0	a	3.6	a	23.2	b

680

TABLE 2: Total Rye Yield, kernel yield, thousand-kernel-weight (TKW), specific weight (SW), area-scaled N_2O emission being the cumulative N_2O emission over the experimental period and the yield-scaled emissions (N_2O; CO_2; $N_2O + CO_2$) of the 3 treatments.

	Treatments		
	Control	MC	SC
Yield (g m^{-2})	818.1 ± 74.3*a*	974.2 ± 24.9*a*	944.3 ± 105.1*a*
Kernel Yield (g m^{-2})	320.1 ± 32.5*b*	416.8 ± 5.4*a*	406.1 ± 56.1*ab*
TKW (g)	26.8 ± 0.8*a*	23.7 ± 0.5*a*	25.9 ± 2.4*a*
SW (kg hl^{-1})	69.8 ± 0.2*a*	70.7 ± 0.4*a*	71.1 ± 0.4*a*
Area-scaled N_2O emission (kg N ha^{-1})	0.74 ± 0.1*b*	0.9 ± 0.1*a*	0.9 ± 0.1*a*
Yield-scaled N_2O emission (kg N Mg^{-1})	8.9e10^{-2} ± 0.01*a*	9.4e10^{-2} ± 0.01*a*	9.3e10^{-2} ± 0.01*a*
Yield-scaled CO_2 emission (kg C Mg^{-1})	607.3 ± 55.8*a*	297.1 ± 6.6*b*	299.4 ± 11.1*b*
Yield-scaled GHG emission (kg CO_2eq Mg^{-1})	2261.5 ± 203.5*a*	1129.9 ± 24.94*b*	1129.6 ± 45.2*b*

*Different characters in the same line indicate significance at the 0.05 level based on one-way ANOVA or t-test (Kernel Yield) The numbers after ± symbol are standard errors of the means (n = 3 or 9). MC and SC are liming treatments (2938,74 VN ha^{-1}).

685 *TABLE 3: Averages calculated for the inorganic and organic soil carbon indices computed for*

686 *each treatment. All abbreviations are defined in the text.*

			Treatment		
Indices	Analisis Type	Units	Control	MC	SC
TOC_{RE}	Rock-Eval®	g/kg	20.2 ± 1.5a	18.9 ± 1.8a	19.3 ± 2.4a
TOC_{EA}	Dry combustion	g/kg	26.7 ± 4.0a	24.4 ± 1.9a	24.4 ± 2.4a
SOM	Dry combustion	g/kg	46.2 ± 7.0a	42.2 ± 3.4a	42.3 ± 4.3a
HI	Rock-Eval®	mg HC/g TOC_{RE}	184.0 ± 18.3b	206.2 ± 9.0a	198.4 ± 19.8ab
OI_{RE6}	Rock-Eval®	mg O_2/g TOC_{RE}	170.9 ± 9.1a	179.3 ± 4.8a	173.5 ± 11.7a
DOC	oxydation	µg C/g dry soil	35.6 ± 11.5b	60 ± 18.8a	53.6 ± 13.5a
DIC	oxydation	µg C/g dry soil	0.5 ± 1.6b	20.23 ± 14.7a	24.52 ± 16.4a

*Different characters in the same line indicate significance at the 0.05 level based on one-way ANOVA. The numbers after ± symbol are standard errors of the means (n = 9). MC and SC are liming treatments (2938,74 VN ha^{-1}).

687

688 *SUPPLEMENTARY TABLE 1: Liming products characteristics.*

689

Treatment	Abbreviation	NV	Particle size (µm)	Marketed by	Quantity/subplot (kg)	Application date
Marine calcium carbonate	MC	52	38	Timac Agro (Calcimer ®)	52.9	19 Oct 2021
Synthetic calcium carbonate	SC	40	50	Roth	49.7	19 Oct 2021

690

691 *SUPPLEMENTARY TABLE 2: ANOVA analysis summary including the degree of freedom for the nominator (DFn) and denominator (DFd) and*

692 *F values for the effects of the liming treatment (Treatment), Time, Block and the interaction of Time and Treatment on the different response*

693 *variables. Log-transformed data were indicated in brackets.*

694

	DFn	DFd	F		DFn	DFd	F		DFn	DFd	F
N_2O (log)				**CO_2 (log)**				**CO_2 + N_2O (log)**			
Block	2	18	2.88	Block	2	18	7.26**	Block	2	18	2.87
Treatment	2	18	22.30***	Treatment	2	18	275.40***	Treatment	2	18	218.66***
Time	27	486	153.39***	Time	27	486	516.77***	Time	27	486	316.20***
Treatment x Time	54	486	3.03***	Treatment x Time	54	486	5.17***	Treatment x Time	54	486	4.03***
WFPS				**pH**				**NH_4^+ - N (log)**			
Block	2	504	120.51***	Block	2	504	17.79***	Block	2	504	2.79
Treatment	2	504	155.20***	Treatment	2	504	1359.09***	Treatment	2	504	2.43
Time	27	504	424.35***	Time	27	504	11.79***	Time	27	504	27.95***
Treatment x Time	54	504	4.398***	Treatment x Time	54	504	5.14***	Treatment x Time	54	504	3.72***
NO_3^- - N (log)											
Block	2	504	1.61								
Treatment	2	504	3.47*								
Time	27	504	270.99***								
Treatment x Time	54	504	4.870***								

695 ***: $p \leq 0.001$; **: $p \leq 0.01$; *: $p \leq 0.5$